# A Nano-In-Nano Approach for Enzyme Immobilization Based on Block Copolymers

Finizia Auriemma[†,*], Claudio De Rosa[†], Anna Malafronte[†,*], Rocco Di Girolamo[†], Chiara Santillo[†], Yuri Gerelli[‡], Giovanna Fragneto[‡], Robert Barker[‡], Vincenzo Pavone[†], Ornella Maglio[†,§], Angela Lombardi[†]

[†] Dipartimento di Scienze Chimiche, Università di Napoli Federico II, Complesso Monte S. Angelo, Via Cintia, 80126 Napoli, Italy

[‡] Partnership for Soft Condensed Matter, Institut Laue-Langevin, 71, avenue des Martyrs, 38000, Grenoble, France

[§] Dipartimento di Biologia IBB-CNR – via Mezzocannone, 16, 80134 Napoli, Italy

*Keywords: Block copolymers, Self-assembly; Nanostructures; Nanoporous surfaces; Enzyme immobilization*

**ABSTRACT:** We have set-up a facile approach for fabrication of supports with tailored nanoporosity for immobilization of enzymes. To this aim block copolymers self-assembly has been used to prepare nanostructured thin films with well-defined architecture containing pores of tailorable size delimited by walls with tailorable degree of hydrophilicity. In particular, we have employed a mixture of polystyrene-*block*-poly(L-lactide) (PS-PLLA) and polystyrene-*block*-poly(ethylene oxide) (PS-PEO) diblock copolymers to generate thin films with a lamellar morphology consisting of PS lamellar domains alternating with mixed PEO/PLLA blocks lamellar domains. Selective basic hydrolysis of the PLLA blocks generates thin films, patterned with nanometric channels containing hydrophilic PEO chains pending from PS walls. The shape and the size of the channels and the degree of hydrophilicity of the pores depend on the relative length of the blocks, the molecular mass of the BCPs, and the composition of the mixture. The strength of our approach is demonstrated in the case of physical adsorption of the hemoprotein peroxidase from horseradish (HRP) using 2,2'-azino-bis(3-ethylbenzothiazoline-6-sulphonic acid) (ABTS) with $H_2O_2$ as substrate. The large surface area, the tailored pore sizes and the functionalization with hydrophilic PEO blocks make the designed nanostructured materials suitable supports for the nanoconfinement of HRP biomolecules endowed with high catalytic performance, no mass-transfer limitations, and long-term stability.

## INTRODUCTION

When an enzyme is immobilized on a support, significant conformational changes may occur, due to the change of the molecular environment of the enzyme with respect to the native state.[1] In particular, the interactions occurring at the interface with the support, modification of hydration shell, steric hindrance between neighboring proteins after immobilization and/or possible enzyme clustering may cause significant conformational changes and, as a consequence, alteration in enzymatic activity.[2,3] Even in absence of conformational changes, adverse orientations, overcrowding, immobilization in a too narrow environment, may seriously hamper the flexibility of the enzyme and/or diffusion of the substrate molecules toward the functional groups, with consequent reduction and/or loss of activity and selectivity.[4]

In general, enzyme immobilization entails either physical adsorption or covalent bonding of the enzyme to the support, by using or not long chain-spacers.[5-8] Immobilization protocols, in turn, may either occur at the surface of a solid carrier, or through trapping of the enzyme inside an open network, or making use of porous media.[6-8] The main applications for which enzyme immobilization is a key issue[9] are bio- and nanobio-technology and in particular biocatalysis,[5,10-12] for fabrication of biosensors[13-15] and/or biofuel cells, in biomedicine and in emerging areas such as nanobiophotonics[16,17] and nanobioelectronics.[18] The added value of exploiting enzyme immobilization for a given application may be envisaged in enhancement of enzyme stability, preservation of catalytic activity and selectivity even in harsh conditions, possibility of re-use, easy separation of the enzyme from the reaction environment.[5,12]

An efficient immobilization strategy requires a rational selection of the supporting material and of the binding protocol, in order to achieve a fine control over confor-

mation, spatial and orientational arrangement of the enzyme on the support.[1] However, the intrinsic complexity of the specific interactions occurring at the interface of an enzyme with an artificial environment (namely the support and the outside reaction medium) not often mimicking the native conditions, makes the set up of an efficient immobilization protocol a difficult task,[19] and no general rules can be established *a priori*. This entails that enzyme immobilization requires the development of methods *ad hoc*, depending on the final application.

Several immobilization methodologies have been proposed to date including protein engineering,[20] chemical modification,[21] inclusion of additives,[22] and immobilization onto or into various matrices.[23-25] In particular, a noticeable progress in enzyme immobilization has been achieved with the use of nanomaterials such as nanoparticles, nanostructured surfaces and nanoporous materials, as these supports enable precise control of the immobilization process, increased rigidity of the enzyme, and resistance to unfolding and deactivation processes, retention of catalytic activity, selectivity and long term stability.[26-29]

Immobilization of enzymes using nanoporous supports is a growing area of research. Numerous efforts have focused on the stabilization of enzymes in nanoporous materials with pores or internal spaces in the range of nanometers.[30-33] The large surface area of nanoporous materials and their opened pore structure can afford improved enzyme loading, which in turn can increase the apparent enzyme activity per unit mass or volume, compared with that of enzymes immobilized onto conventional materials. Several studies have highlighted the stability of enzymes immobilized in various porous matrices, such as carbon, silica, and aluminosilicates,[30,31] able to prevent conformational change or denaturation. Furthermore, the immobilization of biomolecules on surfaces is becoming of particular interest in biochemistry and molecular biology, due to multiple applications in DNA microarray construction and detection of proteins involved in signaling networks in a cell.[34,36]

Block copolymers (BCPs) represent a class of materials that exhibit unparalleled versatility in the construction of nanoporous materials.[37-44] A BCP molecule consists of two or more polymer chains covalently linked at their ends. BCPs constituted by incompatible blocks can give rise to phase separation and formation by self-assembly of nanoscale structures having morphology and characteristic domain size of the incompatible blocks that depend on molecular mass, relative segment length, and the strength of interaction between the blocks, represented by the Flory-Huggins interaction parameter, $\chi$.[45-47] The typical size of the phase separated domains are in the range of 10-200 nm and depends on block length. The exact morphology of phase separated BCPs nanostructures, instead, depends on $\chi$ and the volume fraction of the constituent blocks. In linear AB diblock copolymers, four equilibrium morphologies can be obtained, namely lamellar, hexagonally packed cylindrical, bicontinuous gyroid, and body-centered cubic spherical.[45-47]

Nanoporous materials can be generated by selective removal of a component from a nanostructured block copolymer. Currently, the generation of nanoporous materials from block copolymers relies on a selective etching protocol that does not impair the integrity of the matrix material. Ozonolysis, UV degradation,[42] reactive ion etching (RIE)[43] and chemical etching[39-41,44] are the methods that are commonly used for the removal of minor components to generate nanopores. The resulting materials exhibit the pore size and a pore topology reminiscent of the parent nanostructure, and can be used as nanolithographic masks, separation membranes, nanomaterial template.[37]. To our knowledge, very few examples are reported in literature about the possibility of using BCP based nanoporous thin films as supports to physically absorb proteins and enzymes.[48,49] By immobilizing a biomolecule onto the nanostructured surface of a block copolymer, the presence of pores can enhance the amount of absorbed molecules and can facilitate the retention of the native structure of an enzyme and its activity, thus making the approach suitable as a novel supporting platform for biotechnological applications. The controlled introduction of a specific chemical functionality within the pore space is another critical issue in order to design a porous material useful for an efficient immobilization protocol. In particular, the precise introduction of a specific functionality at pore walls in BCP-based porous materials is important in order to regulate the hydrophilicity of the resulting material, to prevent enzyme aggregation and also to design protocols for the covalent bonding of biomolecules to the obtained porous materials.

Here, we report a simple approach for fabrication of porous block copolymer thin films able to act as support for the physical immobilization of specific biomolecules. In particular, we have designed a nanoporous thin film with well-defined architecture containing functionalized pores delimited by hydrophilic walls, exploiting self-assembly of lamellar block copolymers and the concept of sacrificial block.

The approach has been specifically designed to modify the hydrophilic/hydrophobic characteristics of a given surface, to introduce pores of tailored size at the surface of a support and functional groups inside the pores, with the aim of using them for hosting enzymes without impairing their activity. Although BCPs have been used already for enzyme immobilization,[48,49] our approach is more general, robust and versatile. In this work, we demonstrate its strength when applied to the physical adsorption of horseradish peroxidase (HRP). HRP is a heme protein, which catalyzes the oxidation of various substrates using hydrogen peroxide. HRP is probably the best characterized enzyme, from both mechanistic and structural viewpoints, and the correlations between structural and spectral features of the enzyme, under different conditions, are well

known. Thus, it represents an appropriate system for testing porous block copolymer thin films as suitable support to be used for analytical applications.[50]

## EXPERIMENTAL SECTION

*Materials.* Polystyrene (PS), polystyrene-block-poly(L-lactide) (PS-PLLA) and polystyrene-block-poly(ethylene oxide) (PS-PEO) with number average molecular weights ($M_n$ in Kg $mol^{-1}$) of 83.5, 21.0 (PS)-24.3 (PLLA) and 22.0 (PS)-21.5 (PEO) and molecular mass polydispersity of 1.05, 1.14 and 1.09, respectively, have been purchased from Polymer Source Inc. and used as received. Methanol (99.8%), sodium acetate (99.0%), sodium hydroxide (98%), hydrogen peroxide solution (Fluka, ≥30% RT), 2,2′-Azino-bis(3-ethylbenzothiazoline-6-sulfonic acid) diammonium salt (ABTS) (98.0%, molecular mass 0.5487 Kg $mol^{-1}$) and the protein peroxidase from horseradish (HRP) (total molecular mass 44 Kg $mol^{-1}$, Type VI-A, from Amoracia rusticana, essentially salt-free) have been purchased from Sigma-Aldrich. All the products have been used without further purification. HRP purity, also called Reinheitzahl ($R_z$), estimated from the ratio of absorbance at 403 nm and at 280 nm ($R_z = A_{403}/A_{280}$),[51] amounts to 2.8 ± 0.1, indicating low contamination by other proteins. Silicon (100) substrates (thickness 525 μm) have been purchased from Spi Supplies/Structure Probe Inc. The solvent 1,2-dichloroethane (99.8%) (DCE) and glass supports (size 24x24 mm, thickness 0.13 ÷ 0.16 mm) have been purchased from Carlo Erba Reagents. Silicon and glass substrates have been cleaned with optical tissue and ethanol before use.

*Preparation of thin films and PLLA hydrolysis*. Solutions of PS, PS-PLLA and mixtures of PS-PLLA and PS-PEO at PS-PLLA/PS-PEO ratios of 90/10 and 80/20 w/w have been prepared by dissolving the polymers in 1,2-dichloroethane to yield a total concentration of 0.5% and 1% (w/w) with respect to the solvent. Thin films have been obtained by drop casting or spin coating (RPM 3000 for 30 s) the so obtained solutions on silicon or glass supports. To improve the solid-state morphology, the films containing poly(L-lactide) (PLLA) have been heated to 200 °C and then cooled to room temperature on a hot bench with a gradient temperature. The PLLA removal has been performed placing the thin films into a 0.5 M sodium hydroxide water/methanol (60:40 by volume) solution at 65°C for one min. After removing from the solution, the films have been washed twice with a water/methanol (60:40 by volume) solution, and then dried in a hood at room temperature overnight.

*Horseradish peroxidase catalytic performance (CP) using ABTS as substrate.* Tests of the catalytic performance (CP) of HRP have been performed after incubation of the enzyme for different periods of time on different supports including the bare glass support, the glass support surface-covered with a thin film (thickness 40-80 nm) of the sole PS and the sole PEO, and the 90/10 w/w PS-PLLA/PS-PEO blend before and after etching. In all cases the coverage of the glass support has been performed by spin coating as explained above. All experiments have been performed in triplicate, achieving a high reproducibility. A typical test has been performed as it follows.

*Step 1: Enzyme immobilization.* HRP has been dissolved in distilled water to a final concentration of 18 mg/L. 500 μL of this solution has been deposited onto the supports and incubated for a fixed amount of time. During the incubation time, the samples have been placed on an oscillating stirrer at 10 °C, to minimize solvent evaporation. Then, the enzyme solution has been retrieved from the film surface and the samples have been rinsed with distilled water to remove enzyme molecules that are weakly adsorbed on the surface. Experiments have been performed varying the time of contact between the enzyme solutions and the surfaces. In particular, we have used three different incubation times (30, 90 and 150 min). The decrease of HRP absorbance at 403 nm ($\varepsilon_{403nm}$= 1 $10^5$ $M^{-1}$ $cm^{-1}$) in the solution retrieved from the support with respect to the initial solution used for incubation was 0.6-3%. The HRP signal in the rinsing water, instead, was not spectrophotometrically detectable. We have checked that, in the case of the etched blend, in order to achieve a decrease of HRP absorbance at 403 nm of ≈10%, an incubation time of ≈6 h was necessary. This corresponds to an amount of HRP adsorbed onto the support equal to ≈1.3 ± 0.2 mg $m^{-2}$ (the surface area of the support is 576 $mm^2$). Therefore, the surface density of the HRP molecules deposited onto our nanoporous supports after 6 h incubation time can be estimated to be ≈1.8 $10^{10}$ molecules $mm^{-2}$, yielding an average area per HRP molecule of ≈56 $nm^2$, in good agreement with the results obtained by means of fluorescence measurements for HRP absorbed on Si wafers.[52,53] Moreover, for the tests performed using an incubation time of 90 min, considering that the typical decrease of HRP absorbance at 403 nm in the solution retrieved from the support with respect to the initial solution was less than 1%, the value of surface density of the HRP molecules deposited on the support is less than 1 $10^9$ molecules $mm^{-2}$.

*Step 2: Determination of catalytic performance of immobilized HRP.* The ability of absorbed HRP to catalyze one-electron oxidation by $H_2O_2$ of the dye 2,2′-Azino-bis(3-ethylbenzothiazoline-6-sulfonic acid) diammonium salt (ABTS) into the corresponding radical cation $ABTS^{+\bullet}$ has been tested. The formation of $ABTS^{+\bullet}$ radical cation has been measured spectrophotometrically at 420 nm ($\varepsilon_{420nm}$ = $3.6{\cdot}10^4$ $M^{-1}cm^{-1}$).[54]

A solution of ABTS (2.45 mM) has been prepared in a 50 mM acetate buffer at pH 4.6. Few microliters of $H_2O_2$ solution have been added to the solution in order to obtain a final concentration of 9.75 mM or 0.0975 mM. The reaction has been started by deposition of 500 μL of this solution onto the supports containing absorbed HRP (zero reaction time). We have determined the CP of immobilized HRP by evaluating the amount of the formed radical cation $ABTS^{+\bullet}$ through measurements of the UV-Vis spectra of these solutions after a reaction time of 5 min.

To evaluate the stability of the immobilized enzyme over the time, we have also performed enzymatic assays 7 and 18 days after immobilization. During this time, the supports with the immobilized enzyme have been dried and stored at 4 °C.

*Determination of catalytic performance of free HRP* . Solutions containing ABTS (2.45 mM) and different concentrations of HRP (in the range 0.025-34 nM) have been prepared in a 50 mM acetate buffer at pH 4.6. The reaction has been started by addition of few microliters of $H_2O_2$ solution up to achieve a concentration of $H_2O_2$ in the final solutions equal to 9.75 or 0.0975 mM (zero reaction time). The amount of the product radical cation $ABTS^{+\bullet}$ has been determined by recording UV-Vis spectra of the solutions after a reaction time of 5 min. This quantity corresponds to the CP of free HRP to be compared with the corresponding parameter determined over immobilized HRP.

## RESULTS AND DISCUSSION

**Strategy for preparation of the nanoporous materials.** The strategy exploited to obtain the BCP-based nanoporous materials is reported in Figure 1. We have selected a polystyrene-*block*-poly(L-lactide) (PS-PLLA) and a polystyrene-*block*-poly(ethylene oxide) (PS-PEO) copolymer having nearly identical molecular mass and volume fraction of the PS blocks close to 0.5, in order to create nanostructured thin films characterized by a lamellar morphology. PS-PLLA has been used alone and/or mixed with minor amounts of PS-PEO to prepare thin films from solution by spin coating or drop casting on different surfaces (*vide infra*). Exploiting the good miscibility of PLLA and PEO,[55-57] the final morphology will consist of PS lamellar domains alternating with lamellar domains of PLLA and/or mixed PLLA and PEO blocks (Figure 1a).

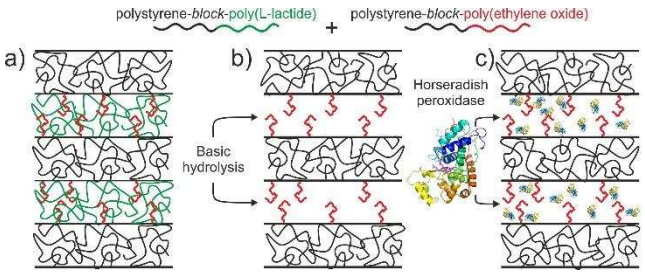


**Figure 1.** Strategy used to obtain BCP based nanoporous materials. (a) The starting material is a nanostructured thin film in lamellar morphology, obtained by mixing polystyrene-*block*-poly(L-lactide) (PS-PLLA) and polystyrene-*block*-poly(ethylene oxide) (PS-PEO) block copolymers. (b) Selective removal of PLLA by basic hydrolysis leaves nanometric channels delimited by PS domains grafted with pendant PEO chains. (c) The porous material is used to immobilize the biomolecule. Only biomolecules penetrating inside the pores are drawn. For clarity, enzyme molecules sticking onto PS domains are not sketched.

Successively, selective basic-catalyzed hydrolysis of the PLLA blocks[39-41] generates nanometric channels delimited by hydrophobic PS domains decorated by carboxylic and hydroxyl end group generated by the cleavage of ester linkage of PLLA blocks,[58] and additional hydrophilic moieties represented by the pendant PEO chains of the PS-PEO component (Figure 1b). The so-obtained nanoporous material is used to immobilize the biomolecule (Figure 1c). Therefore, the rational in the use of PS-PEO as a second component resides in the possibility of tailoring the degree of hydrophilicity of the nanoporous surfaces by simply adjusting the initial composition of the mixture. Additional advantages consist in the ability of PEO to reduce enzyme aggregation and to preserve a more native-like environment for the supported enzyme confined in the nanopores (Figure 1c) even during the dehydration.[1] It is worth noting that the proposed approach can be also extended to immobilization protocols based on the covalent attachment of enzyme molecules to the support, using terminal functionalized PEO blocks.

**Morphological characterization of BCP thin films.** Thin films of the sole PS-PLLA (thickness 40-80 nm) have been prepared by drop casting or spin coating solutions of PS-PLLA in 1,2-dichloroethane at concentration of 0.5% or 1% w/w onto glass slides and/or silicon wafer surfaces. Representative bright-field transmission electron microscopy (TEM) and field emission scanning electron microscopy (FESEM) images of the so obtained thin films are reported in figures 2A and A', respectively. The images exhibit a well-defined phase separated morphology characterized by a disordered array of lamellar domains oriented perpendicular to the glass or silicon surface. In the TEM image (Figure 2A) contrast is due to staining with $RuO_4$, which selectively marks the polystyrene regions. Therefore, the dark regions correspond to stained PS lamellar nanodomains and the bright regions to the PLLA phase. On the contrary, the PS domains appear bright in the FESEM image (Figure 2A'). The average lamellar thickness is estimated to be ≈ 28 ± 3 and ≈ 20 ± 3 nm for PS and PLLA, respectively.

Thin films have been also prepared by drop casting or spin coating 1,2-dichloroethane solutions of mixtures of PS-PLLA and PS-PEO (Figure 1a) at total BCP concentrations of 0.5% or 1% (w/w) by deposition on both glass slides and/or silicon wafer surfaces. Representative bright-field TEM and FESEM images of thin films of the blend (9:1 w/w ratio PS-PLLA:PS-PEO) are reported in Figures 2B and 2B', respectively. There are no significant differences in the resultant morphology compared to the thin films of neat PS-PLLA (Figures 2A and 2A'). The addition of 10 wt% of PS-PEO block copolymer does not alter the lamellar morphology. A well-defined phase separation with a disordered lamellar morphology is observed also in the case of the blend PS-PLLA/PS-PEO. Moreover, also in this case, in the TEM image (Figure 2B) the contrast is provided by staining with $RuO_4$ in order to mark selectively the PS lamellar nanodomains. In the TEM image (Figure 2B), due to the good miscibility of PEO and PLLA,[55-57] the bright lamellar domains correspond to mixed PEO and PLLA components.

The average lamellar thickness of PS and PEO/PLLA domains is similar to that observed in neat PS-PLLA thin films. No significant differences in morphology and lamellar spacing are observed in thin films obtained by drop casting (Figure 2A-B) or spin coating (Figure 2A'-B') for both PS-PLLA and blends.

Thin films of the blend of Figure 2B, B' have been immersed into a 0.5 M sodium hydroxide water/methanol solution at 65°C for one min to remove the poly(L-lactide) blocks (Figure 1b). The temperature used for the basic hydrolysis treatment has been selected close to the glass transition temperature of PLLA (≈ 62 °C). A tilted FESEM image of the etched blend, showing the formation of nanopores, is reported in Figure 3A. The etching treatment does not alter the initial lamellar morphology, as indicated by the comparison of the FESEM images of samples before (Figure 2B') and after the etching treatment (Figure 3A).

The thin film of the etched blend has been also analyzed by TEM without performing any staining procedure (Figure 3A'). A remarkable contrast is present in the TEM micrographs of the etched film demonstrating the effective removal of the PLLA blocks and consequent formation of nanopores. The pronounced contrast in the image of the Figure 3A' is due to PS lamellar domains alternating with the empty channels resulting from PLLA hydrolysis. Since the electron beam is freely transmitted through holes, the scattering and/or adsorption are minimal for the PLLA hydrolyzed regions. No contrast, in fact, is obtained for blend films before the removal of PLLA without resorting to a staining procedure (inset of Figure 3A').

Therefore, the etching treatment results in porous thin films with nanochannels of width 20 nm delimited by PS lamellar domains of width ≈ 28 nm, decorated with pendant PEO chains (Figure 1b). The pores are clearly visible in the tilted FESEM image (Figure 3A). It is worth noting that the etching treatment performed on the neat PS-PLLA thin films results in a remarkable breaking of the initial lamellar morphology due to dewetting (Figure S1), indicating that the presence of PEO component increases the stability of the thin films to water/methanol treatment at 65 °C.

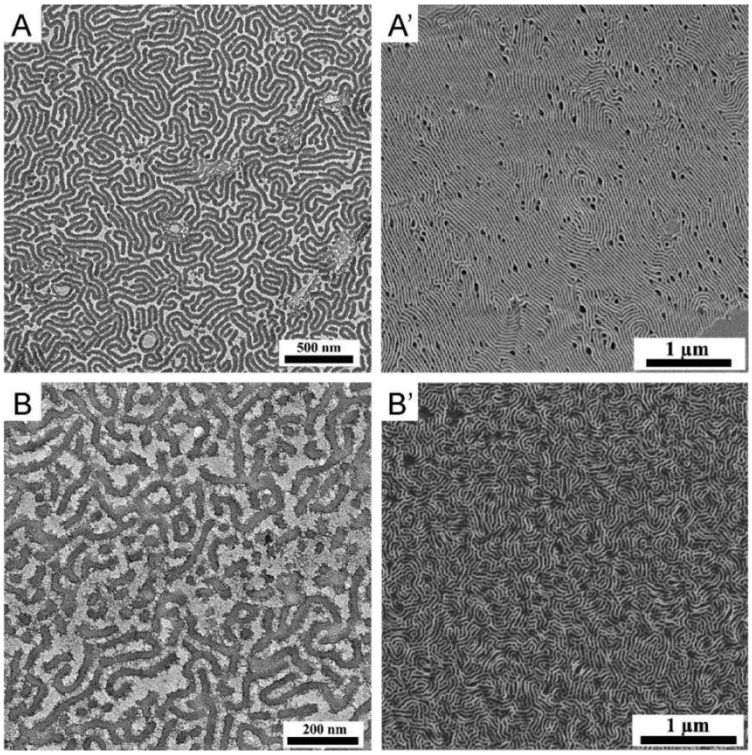


**Figure 2.** Bright-field TEM **(A, B)** and FESEM **(A', B')** images of a thin film of PS-PLLA (A, A') and of the blend PS-PLLA/PS-PEO (B, B'). The films in (A) and (B) have been prepared by drop casting a solution (0.5 wt% in DCE) of PS-PLLA (A) and PS-PLLA/PS-PEO (90/10 w/w) (B) on a glass slide, then the film have been transferred on a TEM grid and stained with $RuO_4$ before observation. The films in (A') and (B') have been prepared by spin coating a solution (1 wt% in DCE) of PS-PLLA (A') and PS-PLLA/PS-PEO (90/10 w/w) (B') on silicon wafers. The typical thickness of these films is 40-80 nm.

**Characterization of the porous material.** The removal of PLLA blocks after etching has been confirmed by Raman measurements. In figure 3B the Raman spectra, acquired in the range 750-1800 $cm^{-1}$, of thin films of blends before (curve a of Figure 3B) and after (curve b of Figure 3B) the etching procedure are reported. The main bands of polystyrene are located at 1000 $cm^{-1}$ (C-C ring breathing mode), 1034 $cm^{-1}$ and 1602 $cm^{-1}$ (tangential ring stretching

mode).[59] These bands are the most intense signals appearing in the Raman spectra. The PS signals are present in both etched and non-etched blend spectra. The relevant PLLA bands appear at 870 and 1770 $cm^{-1}$ and are attributed to the C-COO and C=O stretching modes, respectively.[59] In Figure 3B' and B", the Raman spectra in the regions 900-850 $cm^{-1}$ and 1800-1700 $cm^{-1}$ reveal that the PLLA signals are present in the spectrum of the blend before etching (curves a of Figure 3B-B") and disappear after the etching procedure (curves b of Figure 3B-B"), confirming the removal of PLLA blocks.

Quartz crystal microbalance (QCM) measurements have indicated that ≈ 70 % of the initially present PLLA is removed by etching treatment (Figure S2).

The wettability of the nanoporous films has been determined by contact angle measurements using drops of bidistilled water (Figure S3). The average values of the contact angle (CA) measured on at least 5 independent locations of the sample surface and for three different independent specimens are reported in Table S1. Non-etched PS-PLLA film (Figure S3B) shows a hydrophobic surface with a CA value of (93.0 ± 0.1)°. Introducing the PS-PEO copolymer in the film, the CA value slightly decreases to (84.0 ± 0.1)°, due to the hydrophilicity of PEO blocks (Figure S3C). The etched PS-PLLA film (Figure S3D - D") exhibits a CA of (62.0 ± 0.3)°, confirming the selective removal of PLLA, whereas in the case of the etched blend a CA value of (28.0 ± 0.2)° is achieved, confirming the presence of PEO blocks decorating the PS domains (Figure S3E - E"). Therefore, the incorporation of PEO polyether into the pore space dramatically influences the wettability of the resulting nanoporous material. This demonstrates that our approach allows obtaining surfaces with nanoporous layers of tailored pore size and tailored hydrophilicity with a high degree of reproducibility. In particular the size of the pores may be controlled by the molecular mass of BCP, whereas the hydrophilicity by the relative content of PS-PEO BCP in the blend (Figure S4).

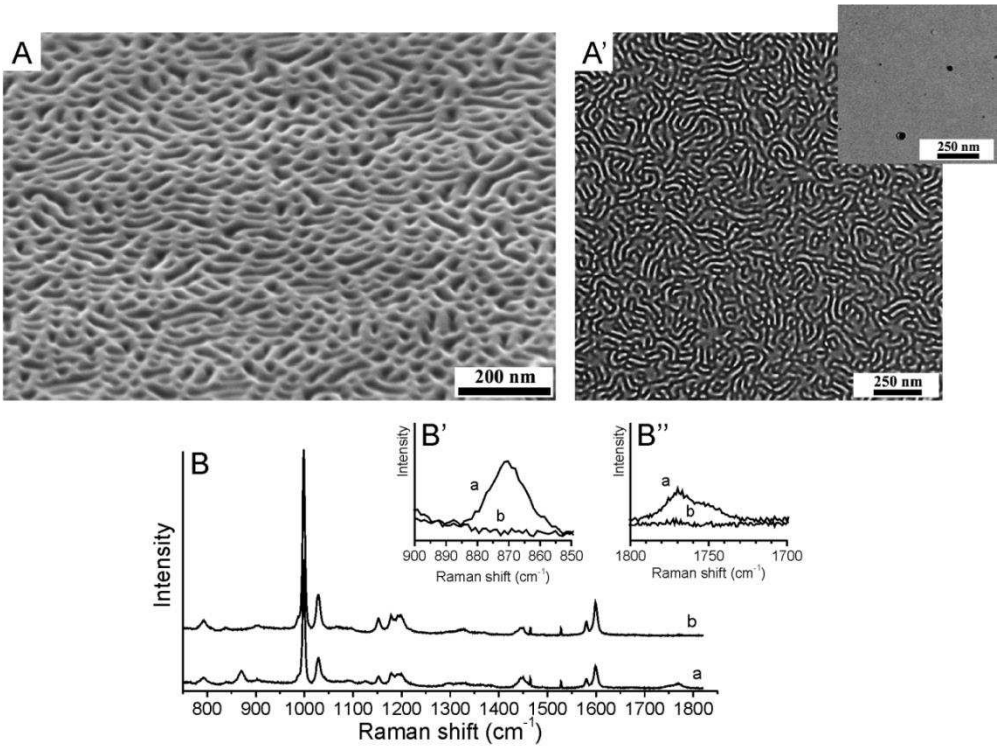


**Figure 3.** Tilted FESEM **(A)** and bright-field TEM **(A')** images of a thin film of the etched blend. The thin films have been prepared by spin coating a solution (0.5 wt% in DCE) of PS-PLLA/PS-PEO (90/10 w/w) and then by immersing them into a basic solution to selectively remove PLLA blocks. No staining procedure has been employed on the film for the TEM observation (A'). The tilt angle of the FESEM image is 66.2°. Inset of *(A')* TEM image of a thin film of the blend before the etching procedure, without staining. **B)** Raman spectra of a thin film of the blend PS-PLLA/PS-PEO before (a) and after (b) the etching procedure in the range 750-1800 $cm^{-1}$. The region 900-850 $cm^{-1}$ and 1800-1700 $cm^{-1}$ are reported in **B'** and **B"**, respectively, in an enlarged intensity scale.

The neutron reflectivity (NR) curves of thin films of blend before and after removal of PLLA are shown in Figure 4A and B, respectively (Supporting Information).[60]

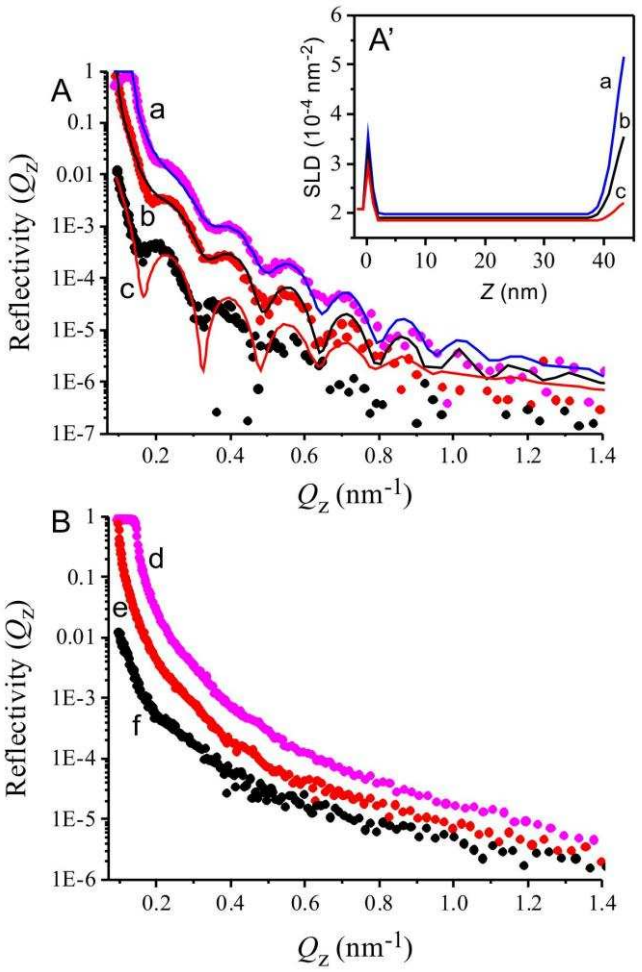


**Figure 4.** Experimental (symbols) and simulated (lines) neutron reflectivity profiles as a function of the wave-vector transfer perpendicular to the surface ($Q_z = 4\pi \sin\theta_i / \lambda$ with $\theta_i$ the angle of incidence and $\lambda$ the neutron wavelength) of thin films of PS-PLLA/PS-PEO (90/10 w/w) blend before (A) and after (B) removal of PLLA in different contrast configurations: D2O (a, d), 4-matched water (4MW) (b, e) and silicon matched water (SiMW) (c, f). Error bars have been removed for clarity. Fits have been obtained according to the parameters listed in Table S2. A') Neutron scattering length density profile (SLD) profiles corresponding to the fits reported in A. Data collected on the D17 reflectometer at the Institut Laue-Langevin.

The lines in Figure 4A correspond to the best common model obtained by the simultaneous fit of the curves measured using three different contrast configurations (see Supporting Information material for details). The fitted parameters are reported in Table S2. The corresponding scattering length density profiles are also shown (Figure 4A'). The samples have been directly prepared on the surface of crystalline silicon wafers comprising a thin amorphous silicon oxide ($SiO_2$) layer at the surface. A two layer model has been used to fit the NR experimental curves from the thin film of blend before the removal of PLLA (Figure 4A, A'). The first layer corresponds to $SiO_2$ at the surface of the silicon supports and the second layer to the polymeric film. The interfacial roughness σ between the $SiO_2$ and the polymeric film is (0.5 ± 0.1) nm. The $SiO_2$ layer has been found to have a thickness equal to (0.9 ± 0.1) nm and contains ≈ 20 % of solvent (Table S2). The solvent in the oxide layer is probably due to pre-treatment of the silicon support by "piranha solution" which makes the oxide layer porous.[61] The values obtained are in good agreement with other reports.[62-64] The interfacial roughness σ between the polymeric film and the solvent is (1.7 ± 0.1) nm. The thin film of blend results (41.1 ± 0.3) nm thick and contains a negligible amount of solvent (≈ 4%, Table S2). The etching process creates a lamellar structure formed by voids and polymer rich regions with the plane perpendicular to the solid surface. This effect strongly affects the reflectivity curves (Figure 4B) since the total reflectivity arises from the incoherent sum of the reflectivity of polymer rich regions plus that of etched surface areas. This, in turn, smears out the Kiessig fringes that were present in the non-etched samples (compare Figures 4A and 4B). The inhomogeneity of the thin film of the etched blends made not possible to use the standard box-model approach (see Supporting Information). As data modeling is not trivial in this case, no fitted lines are shown in Figure 4B.

**Immobilization of enzyme on the nanoporous support.** We have selected a horseradish peroxidase (HRP), as a protein model to generate active surfaces upon adsorption on the BCP nanopouros surfaces. There are various methods for protein immobilization on solid surfaces, including binding to a support (physical adsorption or chemical binding), cross-linking or entrapment. We have performed HRP immobilization by deposition of enzyme solutions onto the supports and incubation for a fixed amount of time. The contact between the enzyme solutions and the supports has been performed for period of time ranging from 30 min to 1.5 h, in order to improve the diffusion and the stabilization of the enzyme.

**Catalytic performance of immobilized HRP.** We have evaluated the catalytic performance of the enzyme HRP immobilized onto our BCP nanoporous surfaces and we have compared the results with those obtained in the case of the same enzyme immobilized on PS thin films and glass slides. The size of the channels of the BCP nanoporous support is ≈ 20 nm, whereas the length of the channels is hundreds nanometers; that is the average area of the pores is well higher than the imprint of a HRP biomolecule lying on a surface (≈ 28 nm²).[52,53,65]

The enzymatic performance of immobilized HRP on the solid surfaces has been assessed in the presence of $H_2O_2$ by means of the oxidation of ABTS into the corresponding radical cation, $ABTS^{+\bullet}$. The catalytic performance (CP) of

HRP immobilized on the different support has been determined as the amount of $ABTS^{+\bullet}$ radical cation produced after 5 min reaction time (see Experimental Section).

In particular, after immobilization, the CP of the enzyme has been evaluated by placing a freshly prepared solution of ABTS and $H_2O_2$ on the surfaces containing immobilized HRP. Three different incubation times (30, 90 and 150 min) have been used. The concentration of the enzyme solution in the incubation step and the experimental conditions during the tests performed to verify the enzyme CP have been kept identical in the three experiments. The UV-Vis spectra of the solutions acquired after 5 min of contact between the ABTS (2.45 mM)/$H_2O_2$ (9.75 mM) solutions and the etched BCP blend, PS and glass slide surfaces containing immobilized HRP are reported in Figure S5A-C, for the three different incubation times, whereas the concentration of the $ABTS^{+\bullet}$ radical cation in the recovered solutions evaluated from the absorbance at 420 nm (Figure S5) are reported in Figure 5A and Table S3.

Using an incubation time of 30 min, no appreciable differences have been observed for the $ABTS^{+\bullet}$ concentration in the solutions retrieved from PS and etched BCP blend (test a of Figure 5A and curves a, b of Figure S5A). Notably, using longer incubation times (tests b, c of Figure 5A and Figure S5 B, C), the intensity of the characteristic peaks of $ABTS^{+\bullet}$ in the solution retrieved from our porous support (curves a of Figure S5B, C) sensibly increases with respect to the solution deposited on the PS surface (curves b of Figure S5B, C). In particular, using an incubation time of 150 min (test c of Figure 5A and Figure S5C), the peak at 420 nm in the case of the etched BCP blend becomes out of scale (curve a of Figure S5C).

The results of Figure 5A and S5 indicate that using a short incubation time (test a of Figure 5A and curves a e b of Figure S5A) the quantity of active HRP immobilized on the PS film and on the etched blend is approximately the same. However, using longer incubation times (test b and c of Figure 5A and Figure S5B, C) the quantity of active enzyme absorbed onto our nanoporous support is higher. We argue that an incubation time of at least 1 h is needed to HRP biomolecules to migrate inside the pores. The green color of the solution reveals the formation of the oxidized product $ABTS^{+\bullet}$ (Figure 5B, C). The color intensity of the solutions, proportional to the concentration of the radical-cation, results higher for the solutions retrieved from our porous support (images c',e' of Figure 5B, C).

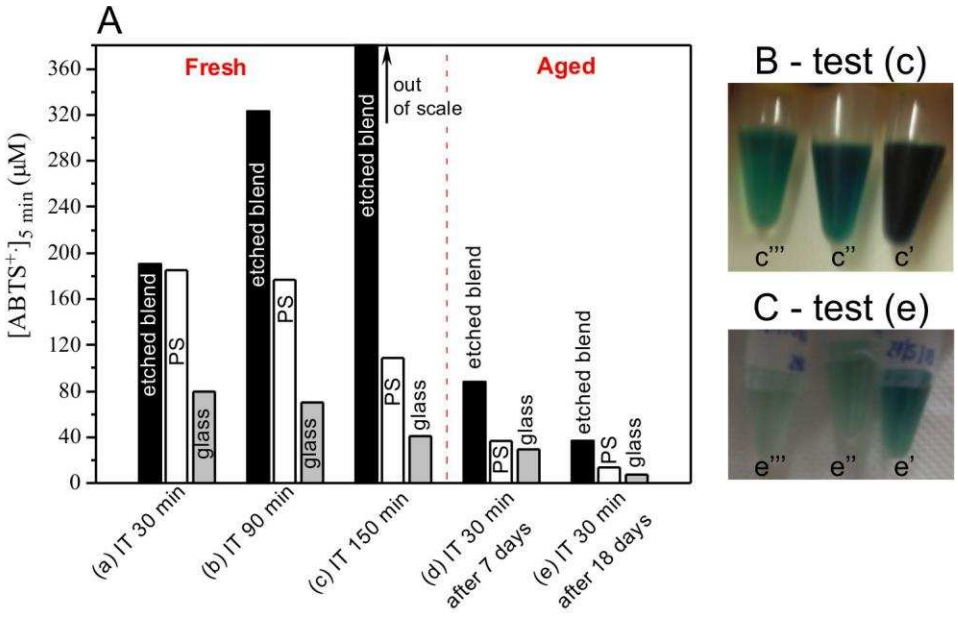


**Figure 5.** A) Concentration of $ABTS^{+\bullet}$ radical-cation evaluated from the ABTS/$ABTS^{+\bullet}$ solutions retrieved after 5 min of contact with the HRP enzyme immobilized on the etched BCP blend, PS and the glass slide. The tests have been performed immediately after the immobilization of HRP (a-c), using different incubation times (IT) of 30, 90 and 150 min, and upon aging the supports for 7 (d) and 18 (e) days after HRP immobilization; in these last two cases the incubation time of HRP is fixed at 30 min. B, C) Photographs of the ABTS/$ABTS^{+\bullet}$ solutions retrieved after 5 min of contact between the ABTS/$H_2O_2$ solutions and the etched blend (c',e'), the PS (c'',e'') and glass slide (c''',e''') in the case of the experiments performed using IT of 150 min (test (c)) and IT of 30 min after 18 days from immobilization (test (e)). The tests have been performed using an ABTS and $H_2O_2$ concentration of 2.45 and 9.75 mM, respectively.

These data suggest that the enzyme retains its catalytic performance after immobilization on the different surfaces and that the quantity of active HRP immobilized on our porous BCP support is higher, if the incubation time is long enough. The result that the incubation protocol of the HRP on our porous surfaces entails a threshold time to significantly differentiate the enzymatic performance of HRP ad-

sorbed on the flat supports suggests that the immobilization process is diffusion limited. In the case of PS and glass supports, indeed, HRP is adsorbed on a flat surface, and only the specific balance of hydrophobic/hydrophilic interactions with the supports plays a key role. In the case of the porous surface of our etched blend, instead, also the diffusion of HRP inside the pores comes into play, since the pore dimensions are comparable with the average dimensions of the enzyme molecules.[52,53]

Parallel tests performed on free HRP in solutions with ABTS/$H_2O_2$ concentration of 2.45 and 9.75 mM, respectively (curve a of Figure S6), reveal that, after 5 min reaction time, the concentration of $ABTS^{+\bullet}$ radical-cation matches the same level obtained by using the etched blend in the test b of Figure 5 (90 min incubation time) with use of a HRP concentration of free enzyme in the solution equal to ≈1 nM (black arrow in Figure S6). Since the estimated amount of immobilized enzyme on the etched support for incubation times of 90 min is of the order of ≈1 $10^9$ molecules $mm^{-2}$ (see Experimental Section), the amount of HRP molecules in contact with 500 µL of solution containing the substrates is also ≈ 1 nM, indicating that immobilization of enzyme on the nanoporous support does not greatly impair the CP of HRP.

It is worth noting that we have also performed catalytic tests using the same condition as Figure 5 and S5, with the enzyme immobilized onto thin films of a PEO homopolymer and of the blend before pores creation (Figure S7). The results demonstrate that the enzyme immobilized onto the thin films of PEO homopolymer (curve d of Figure S7) and non-porous blend (curve e of Figure S7) shows a much lower CP compared to the enzyme immobilized on the other examined surfaces (etched blend, PS and glass slide).

We have also performed the catalytic tests of the enzyme by varying the concentrations of hydrogen peroxide and ABTS (Figure S8). Also in this case, the enzyme immobilized onto our nanoporous support (curves a of Figure S8) shows an increased CP with respect to the enzyme immobilized on PS thin films (curves b of Figure S8) and glass (curves c of Figure S8), and an almost complete preservation of CP, when compared with that of free HRP (red arrow of Figure S6).

Stability of the immobilized enzyme with aging is also critical. Therefore we have characterized the surfaces in terms of long term stability of enzyme CP by measuring the CP of immobilized HRP upon aging the supports for 7 and 18 days after immobilization, using a fixed incubation time (30 min) (tests d, e of Figure 5 A and Figure S5 D, E). As previously discussed, when we perform the test immediately after the enzyme immobilization using an incubation time of 30 min (test a of Figure 5A and Figure S5A), the HRP over the glass slide exhibits the lowest CP (Figure 5A and curve c of Figure S5A) while the HRP immobilized on our porous support (Figure 5A and curve a of Figure S5A) shows CP similar to that immobilized on PS thin film (Figure 5A and curve b of Figure S5 A). In the stability tests, the absorbance decreases with increase of aging time for all the surfaces (tests d, e of Figure 5A and Figure S5 D, E) indicating that the ability of the HRP to catalyze the oxidation of ABTS progressively decreases over the time. However, there is a less pronounced loss in enzyme CP with aging time for the enzyme immobilized on our porous support (compare tests a, d and e of Figure 5A and Figure S5A,D, E). In particular, after 7 days (test d of Figure 5A and Figure S5D), the loss of CP with respect to the freshly prepared support is 54% in the case of the etched blend (curve a of Figure S5D) and 80% and 63% in the case of the PS thin film (curve b of Figure S5D) and the glass slide (curve c of Figure S5D), respectively. Therefore, for non-porous supports there is significant loss in the CP of immobilized HRP. After 18 days (test e of Figure 5A and Figure S5E), the loss of CP for HRP immobilized on our porous support is 81% (19% residual performace, curve a of Figure S5E) while the loss of CP for the HRP immobilized on PS and glass slide is almost total (curves b and c of Figure S5 E). HRP immobilized on non-porous supports displays a more significant decrease in enzyme CP. In other words, enzyme immobilized on non-porous supports is deactivated at a higher rate and our porous BCP matrix is significantly superior in maintaining enzyme CP. It is possible that the porous structure provides an environment that protects enzyme from deactivation. Therefore, the use of porous supports not only yields greater enzymatic CP, but also significantly improves its long-term stability.

Recycling tests of immobilized HRP on the different supports have been also performed. In particular, the supports subjected to 90 min incubation time with HRP have been subjected to consecutive catalytic tests using 500 µL solution of ABTS (2.45 mM) /$H_2O_2$ (9.75 mM), and introducing an intermediate washing step with 500 µL of a 50 mM acetate buffer (pH 4.6) in between each couple of consecutive tests (data not shown). Comparison of the concentration of $ABTS^{+\bullet}$ radical cation obtained in consecutive tests after 5 min reaction time, indicate an almost complete loss of CP of the adsorbed enzyme for the PS and glass supports already after the pristine test, and a much better retention of enzyme CP for the nanoporous supports created by etching our blend, with a CP loss of ≈60% after the third consecutive test.

It is worth noting that physical adsorption of enzyme onto a support is less efficient than covalent immobilization, because part of the protein might easily undergo leaching from the support, with the result that the observed CP is always due to contribution from both the immobilized and solubilized fractions. Notwithstanding, our results demonstrate that after enzymatic tests, the HRP immobilized on our nanoporous BCP supports retain part of initial CP, not only in recycling tests but also after aging. Most importantly, also the initial morphology is retained (data not shown). This entails that the BCP based nanoporous surfaces may be regenerated a repeating number of times through incubation with a new aliquot of enzyme, while maintaining unaltered catalytic performance.

## CONCLUSIONS

Exploiting the partial miscibility of polyethylene oxide (PEO) and poly(L-lactide) (PLLA), and the possibility to easily remove PLLA blocks by basic hydrolysis, we have set up a robust procedure that allows building nanostructured membranes with well-defined architecture containing elongated pores (≈ 20 nm in width) delimited by PEO hydrophilic walls. The large surface area, the tailored pore sizes and the functionalization with hydrophilic PEO blocks make the designed nanostructured material suitable supports for the immobilization of enzymes such as HRP. The use of our porous substrate as confining agent for the HRP improves the catalytic performance of the enzyme without mass-transfer limitations. The total catalytic performance of HRP immobilized onto porous supports is greater than that of HRP immobilized onto flat hydrophilic (glass) and hydrophobic (PS) surfaces and the presence of pores makes the long term stability of immobilized enzyme high. This block copolymer based approach for building nanoporous patterned surfaces is a robust and versatile tool useful not only in applied research such as for fabrication of lab-on-chip biosensors, but also in basic research to study the adsorption mechanism of proteins in constrained environment with controlled geometry at fundamental level.

Finally, we also remark that the present approach has the potential of being easily extendible to usages for which the covalent immobilization of enzymes and biomolecules in general, is required. This can be achieved resorting to the use of a BCP component containing PEO blocks end functionalized (e.g. hydroxyl, ammine or carboxylic groups) which can be exploited in reactions with complementary functional side groups of amino acid residues placed at the outer surfaces of an enzyme (e.g. the amino groups of lysine, or -COOH groups of glutamate) either by direct reaction or using suitable intermediate spacers.

## ASSOCIATED CONTENT

**Supporting Information**. Electron microscopy characterization; Raman microspectroscopy; Contact angle mesurements; Thickness measurements; Neutron reflectometry; UV-Vis experiments; FESEM image of an etched PS-PLLA thin film; Quartz crystal microbalance (QCM) frequency vs. time graphs; Images of the profile of water droplets placed on the surfaces; Table reporting the contact angle (CA) values; FESEM images of thin films of a blend PS-PLLA/PS-PEO containing 20 wt% of PS-PEO before and after the removal of PLLA; Table reporting the fitted parameters of the neutron reflectometry data; Scheme of ABTS/$ABTS^{+\bullet}$ reaction; UV-Visible spectra of the ABTS/$ABTS^{+\bullet}$ solutions recorded in the tests of HRP catalytic performance and table reporting the concentration of $ABTS^{+\bullet}$ radical cation; Free HRP catalytic tests; Additional catalytic data of immobilized HRP by changing the reaction conditions. This material is available free of charge via the Internet at http://pubs.acs.org.

## AUTHOR INFORMATION

### Corresponding Author

* finizia.auriemma@unina.it; anna.malafronte@unina.it

## ACKNOWLEDGMENT

The authors thank Prof. Massimo Lazzari of the University of Santiago de Compostela (Spain) for the collaboration in FESEM characterization, the Italian Agency for New Technologies, Energy and Sustainable Economic Development (ENEA, Portici) for the assistance in performing the angle contact measurements and Prof. Sasso's research group of the University of Naples Federico II for Raman characterization, the Institut Laue-Langevin for beam-time (doi:10.5291/ILL-DATA.9-13-608). This work was supported by Progetto PON/MIUR 01_01585 "Innovative products for monitoring and detoxification/decontamination of nerve agents and explosives in the environment and/or for handling of emergency".

## REFERENCES

[1] Secundo, F. Conformational Changes of Enzymes Upon Immobilization. *Chem. Soc. Rev.* **2013**, *42*, 6250-6261.

[2] Koutsopoulos, S.; van der Oost, J.; Norde, W. Structural Features of a Hyperthermostable Endo-β-1,3-glucanase in Solution and Adsorbed on "Invisible" Particles. *Biophys. J.* **2005**, *88*, 467.

[3] Czeslik, C.; Jackler G.; Royer, C. Driving Forces for the Adsorption of Enzymes at the Water/Silica Interface Studied by Total Internal Reflection Fluorescence Spectroscopy and Optical Reflectometry. *Spectrosc.–Int. J.* **2002**, *16*, 139.

[4] See for instance Talbert, J. N.; Goddard, J. M. Enzymes on Material Surfaces. *Colloids Surf., B* **2012**, *93*, 8-19.

[5] Cantone, S.; Ferrario, V.; Corici, L.; Ebert, C.; Fattor, D.; Spizzo, D.; Gardossi, L. Efficient Immobilisation of Industrial Biocatalysts: Criteria and Constraints for the Selection of Organic Polymeric Carriers and Immobilisation Methods *Chem. Soc. Rev.* **2013**, *42*, 6262-6276

[6] Tufvesson, P. ; Fu, W.; Jensen, J. S.; Woodley, J. M. Process Considerations for the Scale-up and Implementation of Biocatalysis. *Food Bioprod. Process.* **2010**, *88*, 3–11.

[7] Přenosil, J. E.; Kut, Ö. M.; Dunn, I. J.; Heinzle, E. Biocatalysis, 2. Immobilized Biocatalysts. in Ullmann's Encyclopedia of Industrial Chemistry, Wiley-VCH, 2009.

[8] Cao, L. Carrier-bound Immobilized Enzymes, Wiley-VCH, Weinheim, 2005.

[9] Ariga, K.; Ji, Q.; Mori, T.; Naito, M.; Yamauchi, Y.; Abe, H.; Hill, J. P. Enzyme Nanoarchitectonics: Organization and Device Application. *Chem. Soc. Rev.* **2013**, *42*, 6322-6345.

[10] Prakash, S.;Chakrabarty, T.;Singh, A. K.; Shahi, V.K. Polymer Thin Films Embedded with Metal Nanoparticles for Electrochemical Biosensors Applications. *Biosens. Bioelectron.* **2013**, *41*, 43-53.

[11] Cobo, I.; Li, M.; Sumerlin, B. S.; Perrier, S. Smart Hybrid Materials by Conjugation of Responsive Polymers to Biomacromolecules. *Nat. Mater.* **2015**, *14*, 143.

[12] DiCosimo, R.; McAuliffe, J.; Poulose, A. J.;Bohlmann G. Industrial Use of Immobilized Enzymes. *Chem. Soc. Rev.* **2013**, *42*, 6437-6474.

[13] Vigneshvar, S.; Sudhakumari, C.C.; Senthilkumaran, B.; Prakash, H. Recent Advances in Biosensor Technology for Potential Applications - An Overview. *Front Bioeng Biotechnol.* **2016**, *4*, 11.

[14] Willner, I.; Baron, R.; Willner, B. Integrated Nanoparticle-Biomolecule Systems for Biosensing and Bioelectronics. *Biosens. Bioelectron.* **2007**, *22*, 1841-1852.

[15] Bhushan, B. Springer Handbook of Nanotechnology (2010) 3rd ed. (Springer, Heidelberg).

[16] Nagata, M.; Amano, M.; Joke, T.; Fujii, K.; Okuda, A.; Kondo, M.; Ishigure, S.; Dewa, T.; Iida, K.; Secundo, F.; Amao, Y.; Hashimoto, H.; Nango, M. Immobilization and Photocurrent Activity of a Light-Harvesting Antenna Complex II, LHCII, Isolated from a Plant on Electrodes. *ACS Macro Lett.* **2012**, *1*, 296-299.

[17] Lewerenz, H. J. Enzyme–Semiconductor Interactions: Routes from Fundamental Aspects to Photoactive Devices. *Phys. Status Solidi B* **2008**, *245*, 1884-1898.

[18] Wang, J. Biomolecule-Functionalized Nanowires: From Nanosensors to Nanocarriers. *Chem. Phys. Chem*. **2009**, *10*, 1748-1755..

[19] Fersht, A. (1999) Structure and Mechanism in Protein Science. A Guide to Enzyme Catalysis and Protein Folding (W.H. Freeman and Company, New York).

[20] Lee, B.; Vasmatzis, G. Stabilization of Protein Structures. *Curr. Opin. Biotechnol.* **1997**, *8*, 423.

[21] Ó' Fàgàin, C. Enzyme Stabilization—Recent Experimental Progress. Review. *Enzyme Microbiol. Technol.* **2003**, *33*, 137-149.

[22] Chaniotakis, N. A. Enzyme Stabilization Strategies Based on Electrolytes and Polyelectrolytes for Biosensor Applications. *Anal. Bioanal. Chem.* **2004**, *378*, 89-95.

[23] Hernande, K.; Fernandez-Lafuente, R. Control of Protein Immobilization: Coupling Immobilization and Site-Directed Mutagenesis to Improve Biocatalyst or Biosensor Performance. *Enzyme Microb. Technol.* **2011**, *48*, 107.122.

[24] Abad, J. M.; Velez, M.; Santamaria, C.; Guisan, J. M.; Matheus, P. R.; Vazquez, L.; Gazaryan, I.; Gorton, L.; Gibson, T.; Fernandez, V. M. Immobilization of Peroxidase Glycoprotein on Gold Electrodes Modified with Mixed Epoxy-Boronic Acid Monolayers. *J. Am. Chem. Soc.* **2002**, *124*, 12845.

[25] Besanger, T. R.; Chen, Y.; Deisingh, A. K.; Hodgson, R.; Jin, W.; Mayer, S.; Brook, M. A.; Brennan, J. D. Screening of Inhibitors Using Enzymes Entrapped in Sol–Gel-Derived Materials *Anal. Chem.* **2003**, *75*, 2382-2391.

[26] Kim, J.; Grate, J. W.; Wang, *P.* Nanostructures for Enzyme Stabilization. *Chem. Eng. Sci.* **2006**, *61*, 1017-1026.

[27] Ansari, S. A.; Husain, Q. Potential Applications of Enzymes Immobilized on/in Nano Materials: A Review. *Biotechnol. Adv.* **2012**, *30*, 512-523.

[28] Hayat, A.; Catanante, G.; Marty, J. L. Current Trends in Nanomaterial-Based Amperometric Biosensors. *Sensors* **2014**, *14*, 23439-23461.

[29] Saxena, U.; Das, A. B. Nanomaterials Towards Fabrication of Cholesterol Biosensors: Key Roles and Design Approaches. *Biosens. Bioelectron.* **2016**, *75*, 196-205.

[30] Vamvakaki, V.; Chaniotakis, N. A. Immobilization of Enzymes into Nanocavities For the Improvement of Biosensor Stability. *Biosens. Bioelectron.* **2007**, *22*, 2650-2655.

[31] Ravindra, R.; Zhao, S.; Gies, H.; Winter, R. Protein Encapsulation in Mesoporous Silicate: The Effects of Confinement on Protein Stability, Hydration, and Volumetric Properties. *J. Am. Chem. Soc.* **2004**, *126*, 12224.

[32] Küchler, A.; Yoshimoto, M.; Luginbühl, S.; FMavelli, F.; Walde, P. Enzymatic Reactions in Confined Environments *Nat. Nanotechnol.* **2016,** *11,* 409-420.

[33] Hartmann, M.; Jung, D. Biocatalysis with Enzymes Immobilized on Mesoporous Hosts: the Status Quo and Future Trends. *J. Mater. Chem.* **2010**, *20*, 844-857.

[34] Kasemo, B. Biological Surface Science. *Surf. Sci*. **2002**, *500*, 656.

[35] Castner, D. G.; Ratner, B. D. Biomedical Surface Science: Foundations to Frontiers. *Surf. Sci.* **2002**, *500*, 28-60.

[36] Hoheisel, J. D. Microarray Technology: beyond Transcript Profiling and Genotype Analysis *Nat. Rev. Genet*. **2006**, *7*, 200-210.

[37] Hillmyer, M. A. Nanoporous Materials from Block Copolymer Precursors *Adv. Polym. Sci.* **2005**, *190*, 137-181.

[38] Zhang, M.; Yang, L.; Yurt, S.; Misner, M. J.; Chen, J.-T.; Coughlin, E. B.; Venkataraman, D.; Russell, T. P. Highly Ordered Nanoporous Thin Films from Cleavable Polystyrene-block-poly (ethylene oxide). *Adv. Mater.* **2007**, *19*, 1571-1576.

[39] Mao, H.; Arrechea, P. L.; Bailey, T. S.; Johnsonw, B. J. S.; Hillmyer, M. A. Control of Pore Hydrophilicity in Ordered Nanoporous Polystyrene Using an AB/AC Block Copolymer Blending Strategy *Faraday Discuss.* **2005**, *128*, 149-162.

[40] Zalusky, A. S.; Olayo-Valles, R.; Taylor, C. J.; Hillmyer, M. A. Mesoporous Polystyrene Monoliths *J. Am. Chem. Soc.* **2001**, *123*, 1519-1520.

[41] Zalusky, A. S.; Olayo-Valles, R.; Wolf, J. H.; Hillmyer, M. A. Ordered Nanoporous Polymers from Polystyrene–Polylactide Block Copolymers *J. Am. Chem. Soc.* **2002**, *124*, 12761-12773.

[42] Thurn-Albrecht, T.; Schotter, J.; Kastle, G. A.; Emley, N.; Shibauchi, T.; Krusin-Elbaum, L.; Guarini, K.; Black, C. T.; Tuominen, M. T.; Russell, T. P. Ultrahigh-Density Nanowire Arrays Grown in Self-Assembled Diblock Copolymer Templates. *Science* **2000**, *290*, 2126-2129.

[43] Olayo-Valles, R.; Lund, M. S.; Leighton, C.; Hillmyer, M. A. Large Area Nanolithographic Templates by Selective Etching of Chemically Stained Block Copolymer Thin Films. *J. Mater. Chem.* **2004**, *14*, 2729-2731.

[44] Leiston-Belanger, J. M.; Russell, T. P.; Drockenmuller, E.; Hawker, C. J. A Thermal and Manufacturable Approach to Stabilized Diblock Copolymer Templates *Macromolecules* **2005**, *38*, 7676.-7683

[45] Bates, F. S.; Fredrickson, G. H. Block Copolymer Thermodynamics: Theory and Experiment. *Annu. Rev. Phys. Chem.* **1990**, *41*, 525-557.

[46] Hamley, I. W. *The Physics of Block Copolymers;* Oxford University Press: Oxford, 1998.

[47] Fasolka, M. J.; Mayes, Block Copolymer Thin Films: Physics and Applications *Annu. Rev. Mater. Res.* **2001**, *31*, 323-355.

[48] Palacio, M. L. B.; Bhushan, B. Enzyme Adsorption on Polymer-Based Confined Bioinspired Biosensing Surface *J. Vac. Sci. Technol. A* **2012**, *30*, 050607.

[49] Bhakta, S. A.; Benavidez, T. E.; Garcia, C. D. Immobilization of Glucose Oxidase to Nanostructured Films of Polystyrene-block-Poly (2-vinylpyridine) *J. Colloid Interface Sci.* **2014**, 430, 351-356.

[50] Azevedo, A.M.; Martins, V. C.; Prazeres, D. M. F.; Vojinović, V.; Cabral, J. M. S.; Fonseca, L. P. Horseradish Peroxidase: a Valuable Tool in Biotechnology *Biotechnol. Annu. Rev.* **2003**, *9*, 199-247.

[51] Chattopadhyay, K.; Mazumdar, S. Structural and conformational stability of horseradish peroxidase: effect of temperature and pH *Biochemistry* **2000**, *39*, 263-270.

[52] Naves, A. F.; Carmona-Ribeiro, A. M.; Petri, D. F. S. Immobilized Horseradish Peroxidase as a Reusable Catalyst for Emulsion Polymerization. *Langmuir* **2007**, *23*, 1981-1987.

[53] Vianello, F.; Zennaro, L.; Di Paolo, M. L.; Rigo, A.; Malacarne, C.; Scarpa, M. Preparation, Morphological Characterization, and Activity of Thin Films of Horseradish Peroxidase. *Biotechnol. Bioeng.* **2000**, *68*, 488-495.

[54] Childs, R. E.; Bardsley, W. G. The steady-state kinetics of peroxidase with 2,2′-azino-di-(3-ethyl-benzthiazoline-6-sulphonic acid) as chromogen *Biochem. J.* **1975**, *145*, 93-103.

[55] Sheth, M.; Kumar, R. A.; Davé, V.; Gross, R. A.; Mccarthy, S. P. Biodegradable Polymer Blends of Poly(lactic acid) and Poly(ethylene glycol). *J. Appl. Polym. Sci.* **1997**, *66*, 1495-1505.

[56] Baiardo, M.; Frisoni, G.; Scandola, M.; Rimelen, M.; Lips, D.; Ruffieux, K.; Wintermantel, E. Thermal and Mechanical Properties of Plasticized Poly(L-lactic acid). *J. Appl. Polym. Sci.* **2003**, *90*, 1731.

[57] Na, Y.-H.; He, Y.; Shuai, X.; Kikkawa, Y.; Doi Y.; Inoue, Y. Compatibilization Effect of Poly(ε-caprolactone)-b-poly(ethylene glycol) Block Copolymers and Phase Morphology Analysis in Immiscible Poly(lactide)/Poly(ε-caprolactone) Blends. *Biomacromolecules* **2002**, *3*, 1179-1186.

[58] J. Wiggins, S.; Hassan, M.K. ; Mauritz, K.A.;. Storey, R.F Hydrolytic degradation of poly(d,l-lactide) as a function of end group: carboxylic acid vs. hydroxyl. *Polymer* **2006**, *47*, 1960-1969.

[59] The Raman bands have been assigned using Bio-Rad's KnowItAll® ID Expert™ spectroscopy software for the identification of unknown IR & Raman spectra. http://www.bio-rad.com/spectroscopy

[60] Malafronte, A.; Auriemma, F.; Barker, R.; Cioce, C.; Di Girolamo, R. Proposal 2015: Adsorption of undeuterated and deuterated myoglobin on a block copolymer surface with tailored nanopores size and hydrophilicity. Institut Laue-Langevin (ILL) doi:10.5291/ILL-DATA.9-13-608.

[61] Lu, J. R.; Su, T. J.; Thirtle, P. N.; Thomas, R.K.; Rennie, A.R.; Cubitt, R. The Denaturation of Lysozyme Layers Adsorbed at the Hydrophobic Solid/Liquid Surface Studied by Neutron Reflection. *J. Colloid Interface Sci.* **1998**, *206*, 212-223.

[62] Fragneto, G.; Thomas, R.; Rennie, A.; Penfold, J. Neutron Reflection Study of Bovine Beta-Casein Adsorbed on OTS Self-Assembled Monolayers. *Science* **1995**, *267*, 657-660.

[63] McDermott, D.C.; Lu, J. R.; Lee, E. M.; Thomas, R. K.; Rennie, A.R. Study of the Adsorption from Aqueous Solution of Hexaethylene Glycol Monododecyl Ether on Silica Substrates Using the Technique of Neutron Reflection. *Langmuir* **1992**, *8*, 1204-1210.

[64] Fragneto, G.; Lu, J. R.; McDermott, D. C.; Thomas, R. K.; Rennie, A.R. Gallagher, P.D.; Satija, S. K. Structure of Monolayers of Tetraethylene Glycol Monododecyl Ether Adsorbed on Self-Assembled Monolayers on Silicon: a Neutron Reflectivity Study *Langmuir* **1996**, *12*, 477-486.

[65] www.rcsb.org/pdb ID: 1H58, accessed in July 6, 2016.

TOC

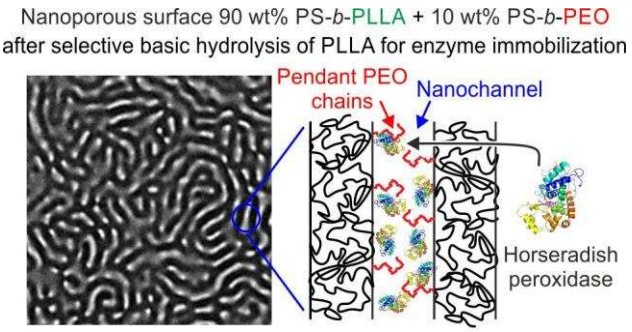
Nanoporous surface 90 wt% PS-b-PLLA + 10 wt% PS-b-PEO
after selective basic hydrolysis of PLLA for enzyme immobilization
Pendant PEO chains
Nanochannel
Horseradish peroxidase